

Inorganic sorbents on the base of magnesium silicates obtained by two synthetic routes

Mykola V. Kravchenko

Institute for Sorption and Problems of Endoecology NAS of Ukraine

Tatiana A. Khodakovska

Institute for Sorption and Problems of Endoecology NAS of Ukraine

Maria F. Kovtun

Institute for Sorption and Problems of Endoecology NAS of Ukraine

Irina V. Romanova (✉ irom@bigmir.net)

Institute for Sorption and Problems of Endoecology NAS of Ukraine

Research Article

Keywords: magnesium silicates, morphology, adsorption, heavy metals, impact of synthetic route and components ratio

Posted Date: June 22nd, 2022

DOI: <https://doi.org/10.21203/rs.3.rs-1753275/v1>

License: © ⓘ This work is licensed under a Creative Commons Attribution 4.0 International License.

[Read Full License](#)

Inorganic sorbents on the base of magnesium silicates obtained by two synthetic routes

M.V. Kravchenko, T.A. Khodakovska, M.F. Kovtun, I.V. Romanova

Institute for Sorption and Problems of Endoecology NAS of Ukraine, Kyiv,
Ukraine, 03164

*E-mail: irom@bigmir.net

Abstract

In the present study three novel inorganic ion exchange materials on the base of magnesium silicates were synthesized by precipitation and hydrothermal sol gel methods with two reagents ratio. Physico-chemical properties of samples were characterized by thermogravimetric and differential thermal analyses, low temperature adsorption/desorption method and transmission electron microscopic studies. It was found that all sorbents were obtained in a form of amorphous layer-structure magnesium silicates with micro- and mesoporous structure. The ion exchange properties of these materials for Cs⁺, Sr²⁺, Cu²⁺, Co²⁺ and Cd²⁺ removing from water solution investigated. Data obtained showed that magnesium silicates had the higher capacity toward the heavy metal cations compared to the radionuclides regardless the method used for synthesis. The sample synthesized with excess of metasilicate exhibited the higher efficiency of heavy metal cations sorption than the sample obtained using equimolar ratio of components. Amongst Langmuir and Freundlich models, Langmuir model fitted well for experimental data received on these adsorbents.

Keywords magnesium silicates · morphology · adsorption · heavy metals · impact of synthetic route and components ratio

* For correspondence

Contact Information: +380976210009

E-mail: irom@bigmir.net

1 Introduction

Large amount of wastes containing inorganic toxicants (radionuclides and heavy metals) have been discharged into the environment over the past few decades [1-4]. Even the small quantities of these pollutants in drinking water, can cause serious health problems of human and animals [5]. Adsorption is the widely employed method used for purification water because of its low costs, convenience, and wide adaptability [6-8]. Among sorbents traditionally applied there are: natural materials [9-12], individual and mixed metal oxides [13-16], sorbents on the carbon base [17] and inorganic compounds such as titanates [18], phosphates [19], silicates [20], etc.

Practice poses well-known requirements to sorbents, first of all, to low cost of their fabrication, to certain parameters of porous structure and to good cations exchange properties. For example, natural silicates after simple modification are the most popular materials used in numerous industrial applications and medicine [21, 22] due to high capacity towards radionuclides and heavy metals [23-25]. The main advantage of synthetic materials including silicates is the possibility to control the textural and surface properties by correlation of synthetic conditions on the stage of mixing reagents and drying precursors [26, 27]. Much works in this field deals with a design the new methods

and improvement existed for obtaining silicates of various metals such as titanium, zirconium, calcium [28-31]. Magnesium silicates as sorbents have received the attention of researchers only last decades.

Magnesium silicate is a compound of magnesium oxide and silicon dioxide with empirical formula $MgO \cdot SiO_2 \cdot nH_2O$, the most common method for its synthesis is via a precipitation reaction between a soluble metal silicate (e.g., sodium orthosilicate, sodium metasilicate, potassium silicate, tetraethyl ortho silicate) and a soluble magnesium salt (e.g., magnesium sulfate, nitrate, or chloride). Silicate anions combine with Mg^{2+} ions in solution forming low solubility magnesium silicates [32-34]. It is known that porous structure and surface of materials obtained depend on the main conditions of synthesis – nature of salts, ratio of components, temperature of drying, etc. Hydrothermal, microwave and ultrasound treatment of precursors positively improve on the properties of materials [35, 36, 37].

The aim of presented work is to synthesize the natural friendly sorbents using low cost reagents (magnesium chloride and sodium metasilicate) with the high surface area and adsorption capacity towards main inorganic toxicants - Cs^+ , Sr^{2+} , Cu^{2+} , Co^{2+} and Cd^{2+} ions. For synthesis has been used the simple methods such as precipitation and sol gel technology with hydrothermal treatment of reagents. The solid phases are investigated by thermogravimetric analysis, transmission electron microscopic studies and low temperature adsorption/desorption method for better understand the morphology of sorbents. The ion-exchange capacity for desired metals ions are evaluated and the impact of method and ratio of components on the main properties of materials are established. Adsorption experiments have been supported by fitting of isotherms by well known theoretical models.

2. Experimental

2.1 Materials

All chemicals used ($MgSO_4 \cdot 9H_2O$, NaOH, CsCl, $SrCl_2 \cdot 6H_2O$, $CoCl_2 \cdot 6H_2O$, $CuNO_3 \cdot 5H_2O$ and $CdNO_3 \cdot 4H_2O$) were of analytical grade and used without further purification. The magnesium content in solutions was controlled by a complexometric titration. Initial and equilibrium concentration of metals in solution for adsorption experiment was measured by atomic absorption spectrometer. The aqueous sodium metasilicate solution of SiO_2/Na_2O molar ratio = 3.1, Na_2O – 9.3 %, SiO_2 – 28 %, density – 1.42 g/L was produced by Ukrainian enterprises and analyzed by acid-basic titration method.

2.2 Synthesis of magnesium silicates

Magnesium silicates ion exchangers were prepared by two methods. The first one consists on drop wise addition of solution (0.5 M) magnesium sulphate (MgSi-1) to sodium metasilicate with equimolar ratio Mg/Si. The precipitate was formed by addition of diluted NaOH solution to the mixture up to pH=11 (precipitation method). The process is carrying out with continuous stirring in a water bath adjusted at room temperature. The mixed solutions were immediately hydrolyzed in deionized water and the precipitates formed were kept in the mother solution overnight. The precipitates were rewashed for several times by distilled water to remove unreacted reagents and the final products were dried at 120 °C, ground, sieved and store at room temperature.

Starting reagents for preparing of samples using sol gel technology were aqueous solutions of magnesium sulphate (0.5 M) and sodium metasilicate used with two equimolar ratio Mg/Si - 1:1 (MgSi-2) and 1:3 (MgSi-3). With continuous stirring, the magnesium sulfate solution was added dropwise to the sodium silicate solution heated up to 60 °C to generate emulsion followed by continuous stirring for 1 h. Then the emulsion was added to a 100 mL Teflon-lined stainless steel autoclave and maintained at 180 °C for 12 h to form hydrogel. The formed hydrogel was repeatedly

filtered with deionized water to remove Na^+ and SO_4^{2-} ions. Finally, the gel was dried at room temperature on air for 24 h to form powder.

2.3 Chemical stability

About 0.05 g of magnesium silicate obtained by two methods were equilibrated with 50 ml solutions of analytical interest at room temperature (25 ± 1 °C) and kept for 24 h with intermittent shaking. The total amount of Mg (mmol/L) dissolved in the solutions was determined using complexometric titration.

2.4 Characterization of magnesium silicates

X-ray diffraction (XRD) patterns were obtained on a DRON – 4-07 diffractometer (LOMO, Russia) using $\text{CuK}\alpha$ excitation ($\lambda=0.15418$ nm) in the 2θ angle range of 5-800 with a 0.020 step. Thermogravimetric analysis (TG-DTA) was carried out in the interval of 20–900 °C in the air with a rate of temperature increase of 10/min on a Derivatograph – Q equipment (Hungary). Specific surface areas and pore size distributions for the synthesized samples were calculated from nitrogen adsorption/desorption curves (NOVA 2200e, Quantachrome, USA) using the Nova Win 2.0 software. The total surface area of the materials S_{total} was calculated by the Brunauer-Emmet-Teller method (BET). The total pore volume (V_{total}) was calculated from the volume of nitrogen adsorbed converted to liquid at a pressure close to $P/P_0 = 1$. To acquire the volume and radii of mesopores (V_{meso} , R_{meso}), Barrett-Joyner-Halenda (BJH) were used. The average pore radii (R_{pore}) was determined from the total pore volume (V_{total}) of the materials and its specific surface area (S_{total}) by equation $R_{\text{pore}} = 2V_{\text{total}}/S_{\text{total}}$. The micropore volume (V_{micro}) was calculated by subtracting the value of V_{meso} from V_{total} . Pore radii distributions were obtained from isotherms in terms of the density functional theory (DFT).

Transmission electron microscope (TEM) investigation was done with a JEM 2100 F microscope (JEOL, Japan).

Sorption properties of the samples of magnesium silicate were studied under static conditions. Concentrations of Cs^+ , Sr^{2+} , Cu^{2+} , Co^{2+} and Cd^{2+} in initial and equilibrium solutions of chlorides and nitrates were measured using Shimadzu AA 6300 (Shimadzu, Japan) atomic adsorption analyzer.

Adsorption capacity (q_e , mmol/g) was calculated by the equations:

$$q_e = (C_0 - C_e) V / m \quad (1)$$

where C_0 and C_e are the initial and equilibrium metal concentration in solution, respectively, mmol/L; V is the aliquot volume (L); and m is the mass of the adsorbent (g).

Experimental data were fitted into the Langmuir and Freundlich models, which are commonly used to describe liquid–solid systems [38] by the following equations:

$$\text{Langmuir: } q_e = Q_0 K_L C_e / (1 + K_L C_e) \quad (2)$$

where q_e is the adsorption capacity (mmol/g); C_e is the equilibrium concentration of the adsorbate (mmol/L); Q_0 is the maximum adsorption capacity of the adsorbent (mmol/g); and K_L is the Langmuir sorption equilibrium constant (L/mmol).

$$\text{Freundlich: } q_e = K_F C_e^{1/n} \quad (3)$$

where K_F ((mmol/g)/(L/mmol)ⁿ) and n are the Freundlich adsorption constants.

To evaluate the correlation between the experimental data and theoretical models, the coefficient of determination (R^2) was calculated.

3 Results and Discussion

3.1 Thermal analysis

All ion exchange materials are obtained and existed in the temperature range 100-600 °C in the amorphous and poorly crystalline phases (weak broad diffraction peaks around $2\theta = 20^\circ$, 35° and 60° , JCPDS 02-1009). Differential thermal and thermogravimetric analyses (DTA and TG) of magnesium silicates obtained by sol gel method with Mg/Si ratio 1:1 (MgSi-2, a) and 1:3 (MgSi-3, b) are given in Fig. 1. Sample MgSi-1 is not presented in Figure because data obtained is similar to MgSi-2. The TG curve of samples (Fig. 1, a, b) show a first loss in weight accompanied by endothermic peaks in DTA curve at 75.2 and 90 °C, respectively, associated with removing water from hydrated magnesium silicate gel [33, 39, 40]. After that a continuous loss in weight is gradually observed up to 650 °C with the peaks ~ 320-330 °C. The second peak is possibly due to the loss of constitution water with transformation amorphous hydroxides to poorly crystalline layer-structure magnesium silicate [39] that is confirmed by small values of weight loss (3-8 % up to 600 °C). The DTA curve of the second sample investigated (MgSi-3, Fig. 1, b) shows the additional endothermic peaks at 475 °C. It is known the thermal decomposition of the layer silicates may be occurs through the anhydrous modification formation in temperature range 400-800 °C [41]. After 900 °C the crystalline layer lattice magnesium silicates dehydroxylates endothermically to form the enstatite MgSiO_3 and silica SiO_2 [39-41].

Fig. 1

3.2 Morphology of magnesium silicates

At first, the porous structure of magnesium silicates synthesized by two routes with various components ratios has been investigated by low-temperature nitrogen adsorption/desorption method, results of these studies are presented in Table 1 and Fig. 2 (a, b). Nitrogen adsorption/desorption isotherms the samples of magnesium silicates according the IUPAC classification [42] belong to the II type with the hysteresis loop of the H3 type (Fig. 2, a). Generally, the precipitated magnesium silicate manifests a relatively high BET specific surface area, total pore volume and volume of meso- and micropores calculated by the BET and BJH methods (MgSi-1, Table 1). Among the samples synthesized by sol gel method MgSi-3 obtained with excess of sodium metasilicate demonstrates the greater parameters than one obtained with equimolar components ratio. It can be noted that parameters of porous structure of MgSi-1 and MgSi-3 are equal to magnesium silicate samples synthesized by more difficult methods with using of expensive reagents [20, 36].

Fig. 2

Table 1 Porosity data for magnesium silicates synthesized by precipitation (MgSi-1) and sol-gel method with ratio of Mg/Si 1:1(MgSi-2) and 1:3 (MgSi-3).

Samples	MgSi-1	MgSi-2	MgSi-3
BET surface area, S_{total} (m^2/g)	597	117	235
Total pore volume, V_{total} (cm^3/g)	0.64	0.25	0.34
Mesopore volume, V_{meso} (cm^3/g)	0.39	0.21	0.26
Micropore volume, V_{micro} (cm^3/g)	0.25	0.04	0.08
Mesopore radius, R_{meso} (nm)	1.7	1.7	1.9
Average pore radius, R_{pore} (nm)	2.1	4.3	2.9

Analyzing the pore size distribution calculated from desorption branches of the isotherms in term of DFT method (presented in Figure 2, b), it is found that in all samples are mesoporous with approx. 1-1.2 nm radii. Sample synthesized by precipitation method (MgSi-1) contains the great amount of micropores supported by data received using low-temperature nitrogen adsorption/desorption method (V_{micro} , Table 2). In the case of samples synthesized by sol gel method it has been indexed the mesopores approx. 2.5 nm that are absent in the structure of the first one.

TEM pictures of the magnesium silicate samples are shown in Figure 3. All samples consist of particles with the size from 10 up to 50 nm. The main difference in texture of samples synthesized by sol gel with the three times excess of metasilicate (MgSi-3, c) is the smaller particles size (~ 20 nm) with the most homogenous structure among samples investigated.

Fig. 3

3.3 Adsorption capacity of silicates

Since the main aim of this study is the removal of heavy metals and radionuclides, at first it has been determined the optimal ratio of the liquid:sorbents (V:m) for experiments, dependence received is presented in Fig. 4, a. Obviously, the adsorption capacity towards copper ions increases in the V:m ratio ranges from 100 to 1000 for all samples, the maximum adsorption capacity is found to be 1.5 mmol/g for sample MgSi-3. Furthermore, to evaluate the adsorption capacity at different initial concentration, 0.025 g of samples was added to 25 mL of metals aqueous solution with concentration of 0.1–10 mmol/L. Resulting mixtures are shaken for 4 h, and left for 1 day at 25 °C, after which the sorbents are removed by means of filtration and the metals content in filtrates are determined.

In order to understand the adsorption mechanism and quantify the adsorption capability experimental data are fitted by two models – Langmuir and Freundlich calculated for copper ions adsorption, results received are shown in Fig. 4, b. The model parameters and coefficients of determination are listed in the Table 2. It is known that Langmuir model describes the homogeneous monolayer adsorption behavior and the Freundlich model describes the multilayer adsorption behavior on the non-homogeneous surface [38].

Fig. 4

Table 2. Langmuir and Freundlich isotherm constants for the adsorption of copper ions onto magnesium silicates.

Samples	MgSi-1	MgSi-2	MgSi-3
Langmuir			
Q_0 (mmol/g)	0.96	0.87	1.70
K_L (L/mmol)	23.8	49.6	28.1
R^2	0.99	0.97	0.99
Freundlich			
$K_F(\text{mmol/g})(\text{L/mmol})^{1/n}$	0.89	0.88	1.34
$1/n$	0.04	0.11	0.11
R^2	0.91	0.91	0.95

The maximum adsorption capacity for Cu^{2+} calculated from Langmuir model is 1.7 mmol/g (experimental 1.7 mmol/g). What's more, Langmuir models fitted better than Freundlich model according to a higher value of R^2 , indicating that the adsorption process is a homogeneous monolayer adsorption.

Data of chemical stability indicated that sample MgSi-3 obtained by sol gel method is stable at investigated pH=7, when the other samples are partially soluble (0.9 and 1.2 mmol/L, respectively).

Figure 5 summarizes the results of Cs⁺, Sr²⁺, Cu²⁺, Co²⁺ and Cd²⁺ adsorption by sorbents on the base of magnesium silicates.

Fig. 5

Data show that all magnesium silicates have the higher capacity toward the heavy metal cations compared to the radionuclides regardless the method used for synthesis. This sequence is in accordance with the hydrated radii of the exchanging ions [43], the ions with smaller hydrated radii easily enter the pores of the exchanger, resulting in higher adsorption. It can be seen from Fig. 5 and Table 3 that the removal rates of metals investigated decrease in the following order: Co²⁺>Cu²⁺>Cd²⁺>Cs⁺=Sr²⁺ (MgSi-1), Cu²⁺>Cd²⁺>Cs⁺>Co²⁺>Sr²⁺ (MgSi-2), Cu²⁺>Cd²⁺>Co²⁺>Cs⁺>Sr²⁺ (MgSi-3). Possible mechanism for the higher selectivity of Cu²⁺ and Co²⁺ ions compared to other metal ions is interpreted by authors [33] considering the great similarity between the ionic radii of Cu²⁺ (0.73 Å), Co²⁺ (0.74 Å) and Mg²⁺ (0.72 Å) leads to including of copper ions in the part of the site of magnesium. Analyzing the maximum of adsorption capacity of magnesium silicates calculated by Langmuir equation (shown in Table 3) it has been noted that sample MgSi-3 can be used as low cost natural friendly sorbent for removing of the inorganic toxicants from water solution.

Table 3. Maximum of adsorption capacity of magnesium silicates sorbents for some cations calculated by Langmuir model.

Sorbent	Cs ⁺	Sr ²⁺	Cu ²⁺	Co ²⁺	Cd ²⁺
MgSi-1	0.30	0.30	0.96	1.51	0.50
MgSi-2	0.51	0.22	0.87	0.3	0.52
MgSi-3	0.6	0.19	1.7	0.79	1.45

4 Conclusions

In this work, three ion exchange materials in the base of magnesium silicate have been obtained by precipitation and hydrothermal sol gel technologies. It was found that all materials obtained were amorphous layer-structure magnesium silicates with micro- and mesoporous structure. Based on low temperature nitrogen isotherms the specific surface area, total pore volume and volume of meso- and micropores calculated by the BET and BJH methods are the greatest for sample obtained by precipitation method. In the case of samples synthesized by sol gel method it is indexed the mesopores approx. 2.5 nm that are absent in the structure of the first one. All samples consist of particles with the size from 10 up to 50 nm. Amongst Langmuir and Freundlich models, Langmuir model fits well for all cations investigated sorption by these adsorbents. It is found that sample MgSi-3 obtained by sol gel method with excess of metasilicate (Mg/Si = 1:3) is chemical stable at pH=7 and has the most homogeneous structure with the smallest particle sizes, the greatest number of pores 2.5 nm sizes, exhibits the highest capacity towards cesium, copper and cadmium ions (0.6, 1.7 and 1.45 mmol/g, respectively) and can be used in adsorption technology for purification of water.

Acknowledgements

Financial support for this study has been provided by National Academy of Sciences of Ukraine within the framework of the target research program “Synthesis and physicochemical studies of composite materials for environmental purposes based on natural and synthetic silicates”, 2022-2024. The authors thank N. I. Danilenko for his help in carrying out TEM measurements and M. M. Tsyba for supporting the porous investigations the materials.

Declarations

Conflict of interest. The authors declare that they have no conflict of interest.

References

1. X. Rena, Ch. Chena, M. Nagatsu, X. Wang, *Chem. Eng. J.* **170**, 395-410 (2011)
2. J. L. Chen, R. Ortiz, T. W. J. Steele, D. C. Stuckey, *Biotechnol. Adv.* **32**(8), 1523-1534 (2014)
3. R. Kumar, M.A. Laskar, I.F. Hewaidy, M. A. Barakat, *Earth. Syst. Environ.* **3**, 83–93 (2019).
4. I. Ihsanullah, M. Sajid, S. Khan, M. Bilal, *Sep. Purif. Technol.* **291**, 120923 (2022)
5. S. Mishra, R. N. Bharagava, N. More, A. Yadav, S. Zainith, S. Mani, P. Showdhary, In: Sobti, R., Arora, N., Kothari, R. (eds) *Environmental Biotechnology: For Sustainable Future*. Springer, Singapore. (2018) https://doi.org/10.1007/978-981-10-7284-0_5.
6. R. J. Drouot, L. Robison, Zh. Chen, T. Islamoglu, O. K. Farh, *Trends Chem.* **1**(3), 304-317 (2019)
7. J. Qu, X. Tian, Zh. Jiang, B. Cao, M. S. Akindolie, Q. Hu, Ch. Fenga, Y. Fenga, X. Meng, Y. Zhang, J. Hazard. Mater. **387**, 121718 (2020)
8. P. Shende, N. P. Devlekar, *Curr. Nanosci.* **17**(6), 819-828 (2021)
9. M.M. Abdellatif, S.M.A. Soliman, N.H. El-Sayed, F. H. Abdellatif, *J. Porous Mater.* **27**, 277–284 (2020)
10. F. Wang, Y. Sun, X. Guo, D. Li, H. Yang, *J. Sol-Gel Sci. Technol.* **96**, 360–369 (2020)
11. K. Sunil, G. Karunakaran, S. Yadav, M. Padaki, V. Zadorozhnyy, R. Krishna Paie, *Chem. Eng. J.* **348**, 678-684 (2018)
12. D.V. Tarnovsky, M.M. Tsyba, L.S. Kuznetsova, T.A. Khodakovska, I.V. Romanova, *J. Chem. Technol.* **29**(2), 192–199 (2021)
13. G. Wang, X. Wang, S. Zhang, Sh. Ma, Y. Wang, J. Qiu, *J. Porous Mater.* **27**, 1515–1522 (2020)
14. W. Wang, A. Wang, *Clays Clay Miner.*, 21-133 (2019)
15. H.J. Song, S. Kim, Y. Cho, *J. Porous Mater.* **27**, 319–328 (2020)
16. I.Z. Zhuravlev, M. F. Kovtun, A.V. Botsman, *Sep. Sci. Technol.* (2021) <https://doi.org/10.1080/01496395.2021.1934024>.
17. P. Vassileva, P. Tzvetkova, L. Lakov, O. Peshev, *J. Porous Mater.* **15**, 593–599 (2008)
18. H. Li, Y. Huang, J. Liu, H. Duan, *Chemosphere*, **282**, 131046 (2021)
19. S. Pan, J. Shen, Z. Deng, X. Zhang, B. Pan, *J. Hazard. Mater.*, **423**, 27158 (2022)
20. Zh. Sun, C. Srinivasakannan, J. Liang, X. Duan, *Ceram. Int.* **45**(4), 4590-4595 (2019)
21. A. Nikolov, H. Nugteren, I. Rostovsky, *Constr. Build. Mater.* **243**, 118257 (2020)
22. K. Maciaszek, D.M.Brown, V. Ston, *Toxicol. In Vitro.* **78**, 105273 (2022)
23. F. A. Dawodu, G. K. Akpomie, *J. Mater. Res. Technol.* **3** (2), 29-141 (2014)
24. V.Yu. Tobilko, L.M. Spasonova, I.A. Kovalchuk, B.Yu. Kornilovych, Yu.M. Kholodko, *Colloids Interfaces*, **3**(1), 41 (2019)

25. M. R. Abass, H. M. Diab, M. M. Abou-Mesalam, *Silicon* **14**, 2555–2563 (2022).
26. I.V. Romanova, S.A. Kirillov, *J. Therm. Anal. Calorim.* **132**, 503-512 (2018)
27. S.A. Kirillov, I.V. Romanova, T.V. Lisnycha, A.V. Potapenko, *Electrochim. Acta.* **286**, 163-171 (2018)
28. S.J. Ahmadi, Y.D. Huang, W. Li, *J. Mater. Sci.* **39**, 1919–1925 (2004)
29. Ch. Cai, H. Wang, J. Han, *Appl. Surf. Sci.* **257**(23) 9802-9808 (2011)
30. G. Qi, X. Lei, L. Li, Ch. Yuan, Y. Sun, J. Chen, J. Chen, Y. Wang, J. Hao, *Chem. Eng. J.* **279**, 777-787 (2015)
31. Z. Wang, W. Liu, Ch. Ling, Q. Xu, Zh. Tang, *J. CO2 Util.* **51**, 101639 (2021)
32. F. Ciesielczyk, A. Krysztafkiewicz, T. Jesionowski, *J. Mater. Sci.* **42**, 3831–3840(2007)
33. I. M. Ali, Y. H. Kotp, I. M. El-Naggar, *Desalination* **259**, 228–234 (2010)
34. A. Spinhaki, G. Petratos, J. Matheis, W. Hater, *Geothermics* **74**, 172-180 (2018)
35. Q. Li, J. Zhang, Q. Lu, J. Lu, J. Li, Ch. Dong, Q. Zhu, *Mater. Lett.* **170**, 167-170 (2016)
36. Zh. Zhao, X. Zhang, H. Zhou, G. Liu, M. Kong, G. Wang, *Microporous Mesoporous Mater.*, **242** 50-58 (2017)
37. M. Dietemann, F. Baillon, F. Espitalier, R. Calvet, M. Greenhill-Hooper, *Powder Technol.*, **356**, 83-96 (2019)
38. K.Y. Foo, B.H. Hameed, *Chem. Eng. J.* **156**, 2–10 (2010)
39. J. Temujin, K. Okada, K. J. D. MacKenzie, *J. Am. Ceram. Soc.* **81**(3) 754–56 (1998)
40. B. Lothenbach, D. Nied, E. L'Hôpital, G. Achiedo, A. Dauzères, *Cem. Concr. Res* **77** 60–68 (2015)
41. N. H. Brett, K. J. D. MacKenzie, J. H. Sharp, *Q. Rev. Chem. Soc.*, **24**, 185-207 (1970)
42. M. Thommes, K. Kaneko, A.V. Neimark, J. P. Olivier, F. Rodriguez-Reinoso, J. Rouquerol, S.W. K. Sing, *Pure Appl. Chem.* **87**, 1051 (2015)
43. I. Persson, *Pure Appl. Chem.* **82** (10), 1901–1917 (2010)

Figures

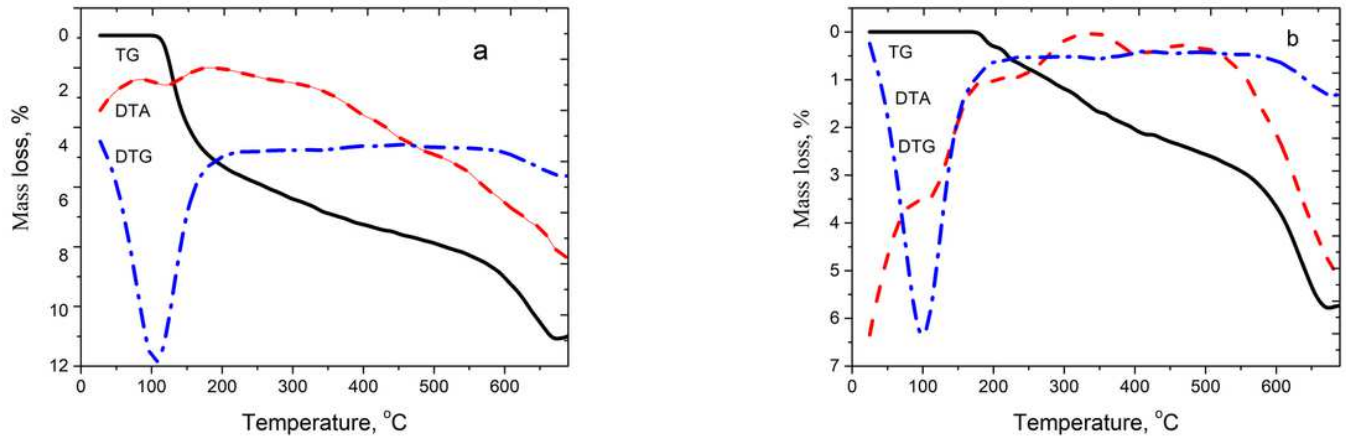


Figure 1

Thermal analysis of magnesium silicates obtained by sol gel method with ratio Mg/Si 1:1 (MgSi-2, a) and 1:3 (MgSi-3, b).

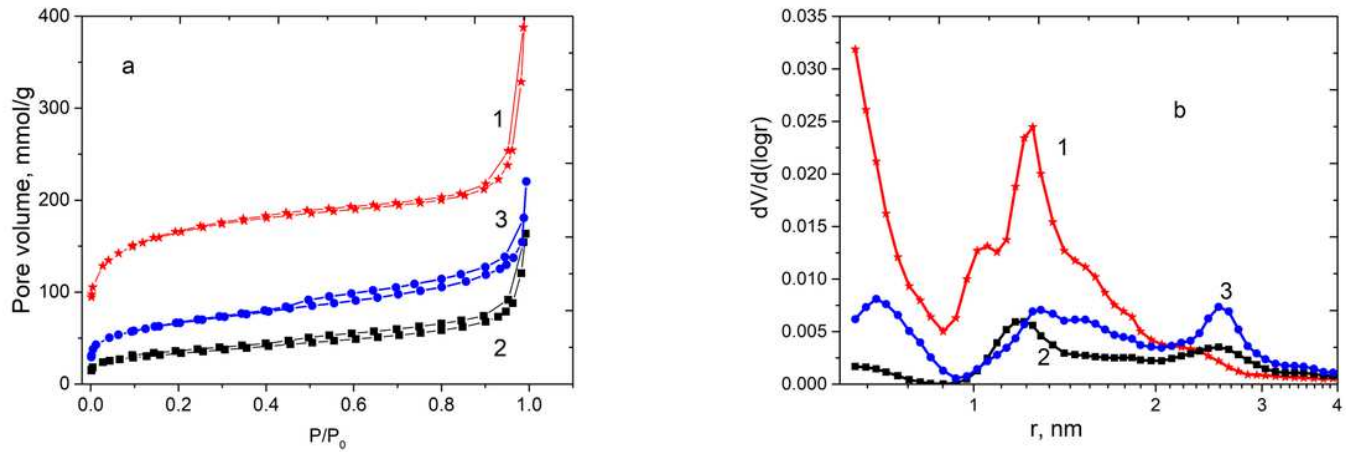


Figure 2

Nitrogen adsorption/desorption isotherms (a) and pore size distributions obtained in term of DFT method for the magnesium silicates synthesized by precipitation MgSi-1(1), and sol gel methods with ratio 1:1 MgSi-2 (2) and 1:3 MgSi-3 (3).

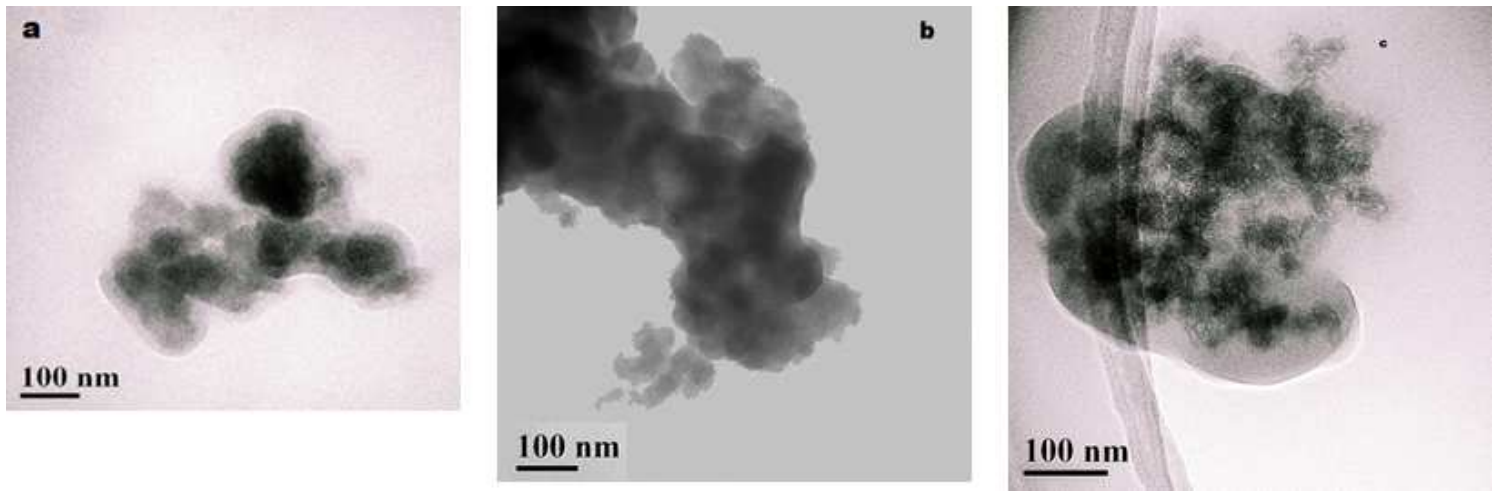


Figure 3

TEM images of magnesium silicates obtained by two methods MgSi-1 (a), MgSi-2 (b) and MgSi-3 (c).

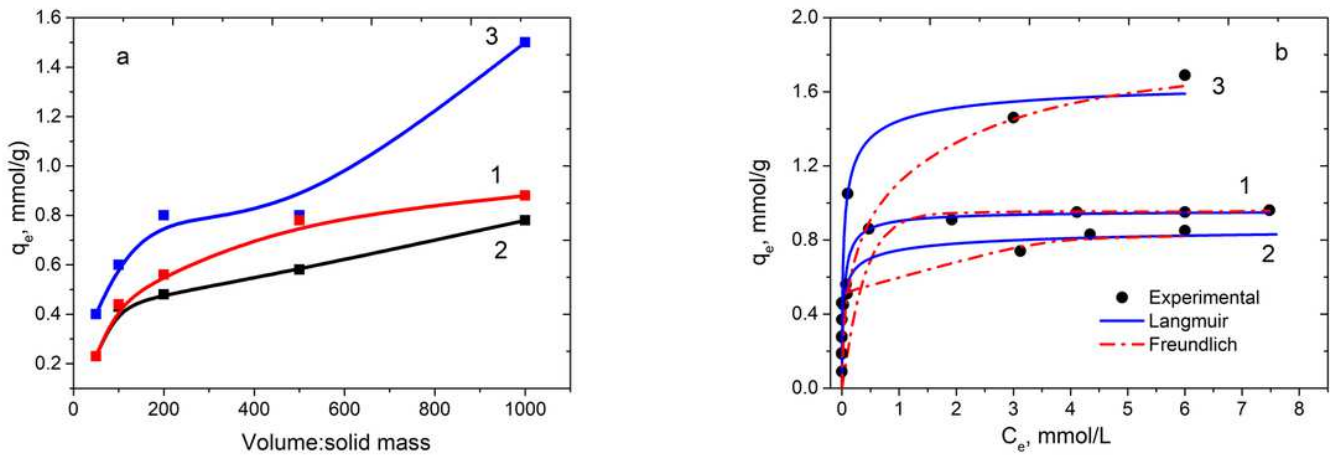


Figure 4

Effect of the ratio between volume and sorbent mass ($V:m$) on adsorption capacity towards Cu^{2+} ($a, C_{\text{Cu}}=4.6 \text{ mmol/L}$), experimental data and plots of Langmuir and Freundlich isotherm models for the adsorption of copper by samples: MgSi 1 (1), MgSi 2 (2) and MgSi 3 (3).

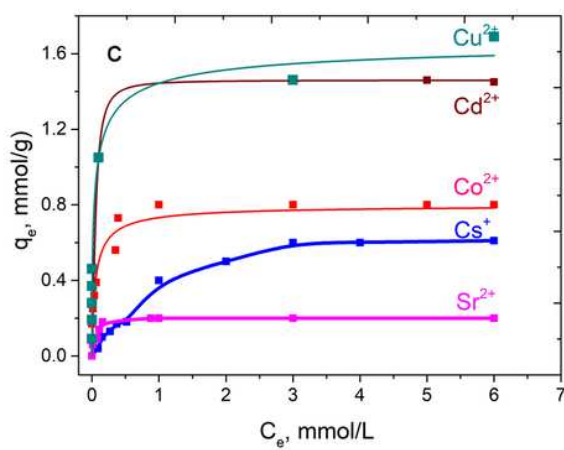
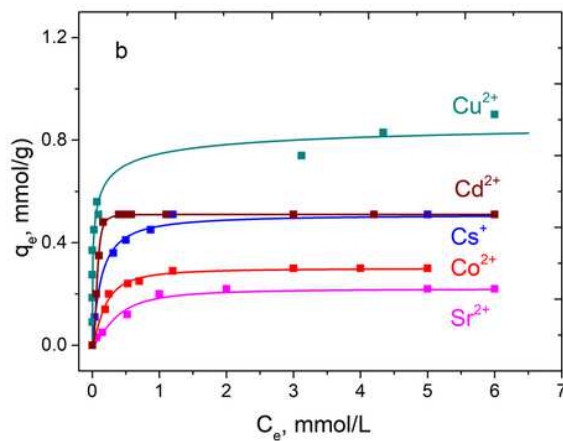
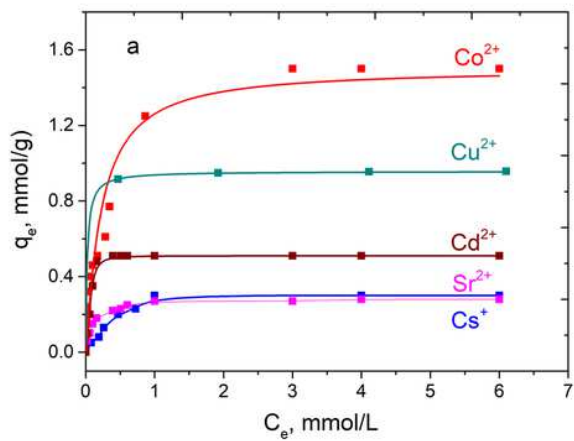


Figure 5

Sorption isotherms for Cs^+ , Sr^{2+} , Cu^{2+} , Co^{2+} and Cd^{2+} adsorbed onto the samples MgSi-1 (a), MgSi-2 (b) and MgSi-3 (c).